Journal of the Korean Nuclear Society
Volume 30, Number 5, pp.470~484, October 1998

《Technical Note》

Deterministic Fracture Mechanics Analysis of Pressurized Thermal Shock

M. J. Jhung and Y. W. Park
Korea Institute of Nuclear Safety
19 Kusong-dong, Yusong-gu, Taejon, 305-338 Korea

(Received May 12, 1997)

Abstract

An analysis program for the evaluation of pressure vessel integrity under pressurized thermal shock (PTS) is developed. For given material properties and transient history such as temperature and pressure, the stress distribution is calculated and then stress intensity factors are obtained for a wide range of crack sizes. The stress intensity factors are compared with the fracture toughness to check if cracking is expected to occur during the transient. Using this program a round robin problem of PTS during a small break loss of coolant transient has been analyzed as a part of the international comparative assessment study. The allowable maximum reference nil-ductility transition temperatures are determined for various crack sizes.

1. Introduction

A nuclear reactor pressure vessel, which contains fuel assemblies and reactor vessel internals, is a very important structure because it keeps coolant of high temperature and pressure during normal operation. Therefore, it is designed and manufactured according to strict regulations and studies on its integrity are under going actively.

Since the Rancho Seco transient in 1978, a pressurized thermal shock has been designated as a severe safety issue. Pressurized thermal shock involves a transient in which severe overcooling causes a thermal shock to the vessel, while the pressure is either maintained or the system is repressurized during the transient. The thermal stress resulting from the rapid cooling of the vessel walls in combination with the pressure stress from either maintaining system pressure or repressurization of the system results in large tensile stresses which are at a maximum at the inside surface of the vessel. The concern was that the combination of the pressure stress and thermal stress along with a decrease in fracture toughness due to the material temperature falling below its nil ductility transition temperature could cause through-wall propagation of a relatively small crack. Therefore, it is necessary to evaluate a structural integrity of a reactor pressure vessel under pressurized thermal shock event.

In this study, theory of fracture mechanics for the pressurized thermal shock is investigated and a

calculation routine for the evaluation of the pressure vessel under pressurized thermal shock is developed. For given material properties, transient history such as temperature and pressure, and postulated flaw, the stress distribution is calculated and then stress intensity factors are obtained for a wide range of crack sizes. The stress intensity factors are compared with the material fracture toughness values to check the crack growth during the transient (Figure 1).

Also, using this program a round robin problem of PTS during a small break loss of coolant transient has been analyzed as a part of the international comparative assessment study. The allowable maximum reference nil-ductility transition temperatures are determined for various crack sizes.

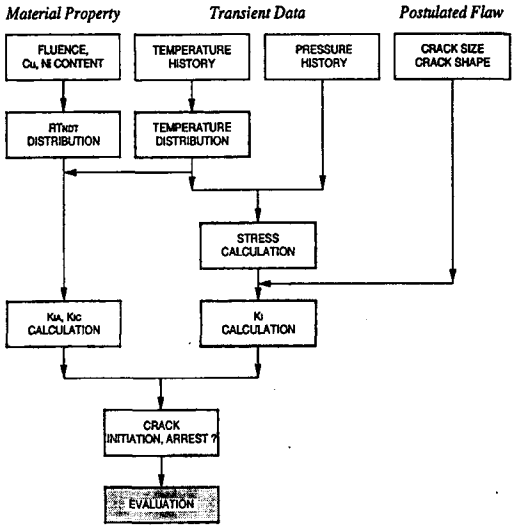

Fig. 1. Evaluation Procedure for Pressurized Thermal Shock

2. Calculation of Temperature and Stress Distributions

2.1. Temperature Distribution

Considering a very long cylindrical vessel with uniform fluid temperature, the temperature distribution in the vessel wall $T(r, t)$ is assumed to be governed by the ordinary differential equation [1]

$$\rho c T_t - K\left(\frac{1}{r}T_r + T_{rr}\right) = 0 \qquad (1)$$

subject to initial condition and boundary conditions assuming insulation at outside vessel wall

$$\begin{aligned} &T(r,\ 0) = T_0 \\ &T_r(r_o,\ t) = 0 \\ &-KT_r(r_i,\ t) = h[T_c(t) - T(r_i,\ t)] \end{aligned} \qquad (2)$$

where T_0 is the initial coolant temperature, T_c the coolant temperature, K the heat conductivity of the material, h the heat transfer coefficient between the coolant and vessel material, ρ the material density, c the material specific heat, r_o the outer radius, r_i the inner radius and t the time. Subscript r represents the differentiation with respect to radial coordinate.

The finite difference equations for N radial points, at distance Δr apart, across the vessel are [2]

$$\text{for } n=1;\quad T_1^{t+\Delta t} = \left[1 - \frac{\Delta tK}{\rho c(\Delta r)^2}\left(1+\frac{\Delta r}{r_i}\right) - \frac{\Delta th}{\rho c(\Delta r)}\right]T_1^t + \frac{\Delta tK}{\rho c(\Delta r)^2}\left[\left(1+\frac{\Delta r}{r_i}\right)T_2^t + \frac{\Delta rh}{K}T_c^t\right] \qquad (3\text{-}1)$$

for $1 < n < N$;

$$T_n^{t+\Delta t} = \left[1 - \frac{\Delta tK}{\rho c(\Delta r)^2}\left(2+\frac{\Delta r}{r_n}\right)\right]T_n^t + \frac{\Delta tK}{\rho c(\Delta r)^2}\left[\left(1+\frac{\Delta r}{r_n}\right)T_{n+1}^t + T_{n-1}^t\right] \qquad (3\text{-}2)$$

and for $n = N$;

$$T_N^{t+\Delta t} = \left[1 - \frac{\Delta tK}{\rho c(\Delta r)^2}\right]T_n^t + \frac{\Delta tK}{\rho c(\Delta r)^2}T_{n-1}^t \qquad (3\text{-}3)$$

For stability in the finite difference operation, we must choose Δt for a given Δr such that both

$$\frac{\Delta tK}{\rho c(\Delta r)^2}\left(2+\frac{\Delta r}{r_i}\right)\le 1 \tag{4-1}$$

and

$$\frac{\Delta tK}{\rho c(\Delta r)^2}\left(1+\frac{\Delta r}{r_i}\right)+\frac{\Delta th}{\rho c(\Delta r)}\le 1 \tag{4-2}$$

are satisfied.

Since a large variation in coolant temperature is considered, the thermal conductivity K(btu/hr-ft-°F) and the thermal diffusivity k(ft^2/hr) can be determined from the ASME Code Section III [3]. A linear regression analysis of the tabular values resulted in the following expressions :

SA508 Class 3 :

$$K = 21.309 + .88517\frac{T}{10^2} - .19641\frac{T^2}{10^4} + .91496\frac{T^3}{10^8} \tag{5}$$

$$k = .43040 - .14836\frac{T}{10^3} - .45642\frac{T^2}{10^7} + .16109\frac{T^3}{10^{11}} \tag{6}$$

SA533B Class 1 :

$$K = 21.303 + .16033\frac{T}{10^1} - .29469\frac{T^2}{10^4} + .12344\frac{T^3}{10^7} \tag{7}$$

$$k = .42549 + .68456\frac{T}{10^4} - .51640\frac{T^2}{10^6} + .28578\frac{T^3}{10^9} \tag{8}$$

where T is in degrees Fahrenheit.

2.2. Stress Distribution

2.2.1. Thermal Stress

The thermal stress distribution is calculated from [4, 5]

$$\sigma_{T,hoop}(r,t) = \frac{\alpha E}{1-\nu}\left[\frac{1}{r^2}\int_{r_i}^{r} T(r,t)rdr - T(r,t) + \frac{1}{r^2}\frac{r^2+r_i^2}{r_o^2-r_i^2}\int_{r_i}^{r_o} T(r,t)rdr\right] \tag{9}$$

$$\sigma_{T,axial}(r,t) = \frac{\alpha E}{1-\nu}\left[\frac{2}{r_o^2-r_i^2}\int_{r_i}^{r_o} T(r,t)rdr - T(r,t)\right] \tag{10}$$

where E(ksi) is Young's modulus, α (ft/ft °F) the coefficient of thermal expansion, and ν Poisson's ratio. Poisson's ratio is taken to be constant while α and E are evaluated as a function of the average temperature T_{avg} across the vessel [3] as follow :

$$T_{avg} = \frac{2}{r_o^2-r_i^2}\int_{r_i}^{r} T(r,t)rdr \tag{11}$$

$$E = 27.968 - .53395\frac{T}{10^2} + .65784\frac{T^2}{10^5} - .92201\frac{T^3}{10^8} \tag{12}$$

SA508 Class 3 :

$$\alpha = 10^{-6}\times\left(6.2996 + .18464\frac{T}{10^2} + .32482\frac{T^2}{10^6} - .44579\frac{T^3}{10^9}\right) \tag{13}$$

SA533B Class 1 :

$$\alpha = 10^{-6}\times\left(6.8420 + .23285\frac{T}{10^2} - .14897\frac{T^2}{10^5} + .58824\frac{T^3}{10^9}\right) \tag{14}$$

2.2.2. Pressure Stress

The stresses due to internal pressure $\sigma_p(r, t)$ are calculated using the following equations [4, 5] :

$$\sigma_{p,hoop}(r, t) = p(t)\ \frac{r_i^2}{r_o^2 - r_i^2}\times\frac{r_o^2 + r^2}{r^2} \tag{15}$$

$$\sigma_{p,axial}(r, t) = \frac{1}{2}\ \frac{p(t)r}{r_o - r_i} \tag{16}$$

3. Fracture Mechanics Analysis

3.1. Stress Intensity Factor

Stress intensity factor for the flaw is calculated

from the membrane and bending stresses determined from stress analysis at the flaw location using the following equation [6]:

$$K_I = \sqrt{\pi \frac{a}{Q}} (M_m \sigma_m + M_b \sigma_b) \quad (17)$$

where σ_m is the membrane stress (ksi), σ_b the bending stress (ksi), M_m the correction factor for membrane stress, M_b the correction factor for bending stress, a the flaw depth for surface flaw and Q the flaw shape factor. The stresses σ_m and σ_b are determined from Fig. A 3200-1 of ASME Code Section XI, Appendix A [6], M_m and M_b from Fig. A 3300-2~5, and Q from Fig. A 3300-1.

3.2. Fracture Toughness

The fracture toughness of the material is defined by two properties K_{IA} and K_{IC}, which represent critical values of the stress intensity factor. K_{IA} is based on the lower bound of crack arrest critical K_I values measured as a function of temperature. K_{IC} is based on the lower bound of static initiation critical K_I values measured as a function of temperature. Lower bound K_{IA} and K_{IC}, versus temperature curves from tests of SA-533 Grade B Class 1, SA-508 Class 2, and SA-508 Class 3 steel are provided in Fig. A 4200-1 of [6] and can be represented as [7] :

$$K_{IC} = 33.2 + 2.806e^{0.020(T-RT_{NDT}+100)} \quad (18)$$

$$K_{IA} = 26.8 + 1.233e^{0.0145(T-RT_{NDT}+160)} \quad (19)$$

where RT_{NDT} is the reference nil-ductility transition temperature which is given by the following expression :

$$RT_{NDT} = RT_{NDT0} + \Delta RT_{NDT} \quad (20)$$

The initial RT_{NDT}, RT_{NDT0}, is the reference temperature for the unirradiated material and ΔRT_{NDT} is the mean value of the adjustment in reference temperature caused by irradiation and is calculated as follows :

$$\Delta RT_{NDT} = CF \times f^{0.28-0.101 \log f} \quad (21)$$

CF (°F) is the chemistry factor, a function of copper and nickel content, determined from Regulatory Guide 1.99, Rev.2 [8]. The neutron fluence in the vessel wall, $f(10^{19}\text{n/cm}^2, E > 1$ MeV), is determined as follows :

$$f = f_{surf}\, e^{-0.24a} \quad (22)$$

where f_{surf} (10^{19}n/cm^2, E > 1 MeV) is the calculated value of the neutron fluence at the inner wetted surface of the vessel at the location of the postulated defect and a (in inches) is the depth into the vessel wall measured from the vessel inner surface.

4. Development of Program

4.1. Critical Crack Depth Diagram

Using the stress and temperature profiles as a function of time following the postulated incident, stress intensity factors are calculated for various penetration depths. The crack arrest K_{IA} and crack initiation K_{IC} fracture toughness profiles are also determined using the irradiated fracture toughness data. For each time during the transient, the variations of K_I, K_{IC} and K_{IA} through the thickness are determined as shown in Figure 2. The crack penetration at which the calculated stress intensity factor exceeds K_{IC} profile corresponds to the critical crack size for initiation (a_c) and the penetration at which the stress intensity factor goes below the K_{IA} curve corresponds to the

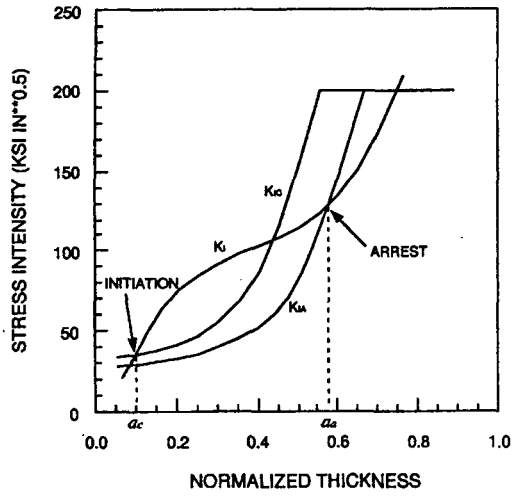

Fig. 2. Determination of Critical Flaw Sizes

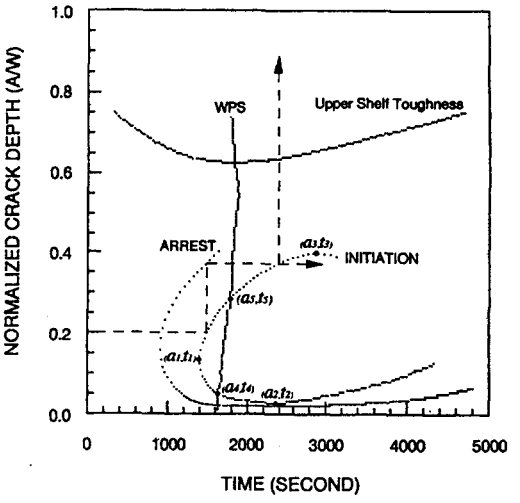

(a_i,t_i) : (crack depth, time)
1 : first initiation
2 : minimum depth for initiation
3 : maximum depth for initiation
4 : minimum depth for initiation considering WPS
5 : maximum depth for initiation considering WPS

Fig. 3. Typical Critical Crack Depth Diagram

critical crack size for arrest (a_a). Graphs of a_c and a_a versus time, called a critical crack depth diagram, are then prepared as shown in Figure 3. A critical crack depth diagram consists of curves for initiation ($K_I = K_{IC}$), arrest ($K_I = K_{IA}$), and upper shelf toughness (K_I = 200 ksi$\sqrt{\text{in}}$). The behavior of a crack initiation and arrest can be predicted from this diagram for the assumed crack following a postulated transient. If there is a crack with a/w = 0.20, it is initiated twice following the dotted line resulting in through-wall propagation. In Figure 3, (a_1, t_1) is a crack size and time when a first initiation occurs and $a_2 \sim a_3$ is the range of the crack sizes which can be initiated during a postulated transient. If a crack is so small or large and is beyond this range, it is not initiated. The smallest value of a_c, a_2, is used for comparison with acceptance criteria.

4.2. Warm Prestressing

Several studies [9, 10] have shown that the fracture toughness can be significantly increased at low temperatures if the material is prestressed at a higher temperature. A conservative method is formulated to use this warm prestressing effect in the fracture mechanics of pressure vessels under thermal shock. This method uses the basic premise that a crack will not initiate when the stress intensity factor is dropping with time or constant, whether or not the temperature is dropping.

According to classical linear elastic fracture mechanics, flaws will begin to initiate when K_I exceeds K_{IC}. However, according to the conservative warm prestressing principle, K_I must exceeds K_{IC} before the maximum K_I occurs, for initiation to take place; otherwise initiation cannot occur when K_I is dropping with time. For each flaw depth, the time (θ_{max}) for the peak K_I to occur is determined. The variation of θ_{max} with crack depth is then plotted on the same graph as a_c and a_a versus time. Therefore warm prestressing curve ($dK_I/dt = 0$) is also included in the critical crack

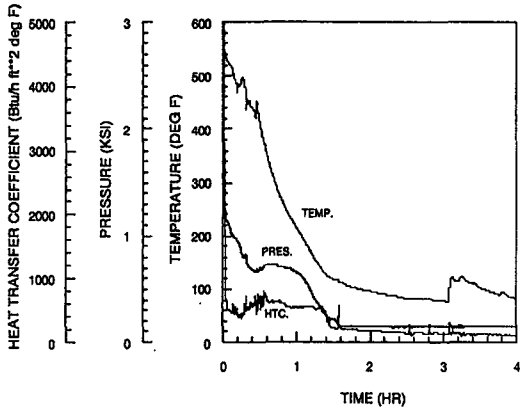

Fig. 4. Pressure, Temperature and Heat Transfer Coefficient Histories

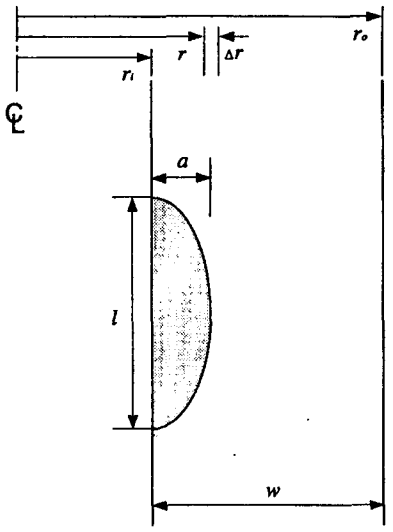

Fig. 5. Postulated Surface Crack

depth diagram. For a given flaw depth, if the θ_{max} curve is crossed before a_c curve, no initiation will occur because of warm prestressing. In Figure 3, a crack (a/w = 0.20) is initiated once, arrested at about a/w = 0.375 and not initiated again. Considering a warm prestressing effect, the intersections of the θ_{max} curve and a_c curve define the range of flaw sizes that would initiate. In Figure 3, $a_4 \sim a_5$ is the range of the crack sizes which can be initiated during a postulated transient. The minimum flaw (a_4) that would initiate is determined by the lowest intersection of the θ_{max} and the a_c curves; the maximum flaw (a_5) that would initiate is determined by the highest intersection of the θ_{max} and the a_c curves.

5. Round Robin Problem

5.1. Problem Definition

The reactor pressure vessel is loaded by emergency cooling transients due to assumed leaks [11]. Transient is due to a small break loss of coolant accident. The primary pressure and the averaged fluid temperatures as well as heat transfer coefficients in the downcomer are presented in Figure 4. For this transient axial symmetric loading conditions with no change in axial position are assumed.

Table 1. Vessel Parameters for the Analysis

vessel thickness	9.57 inches
vessel inner radius	98.425 inches
material	SA 508 Class 3
Cu content	0.30 weight %
Ni content	0.75 weight %
initial RT_{NDT}	20°F

Circumferential and axial semielliptical surface cracks of depth a / w = 0.06 are postula-ted. Various aspect ratios are assumed to investigate the influence of the aspect ratio (Figure 5).

The temperature and stress distribution in the vessel wall will be shown according to the given material properties (Table 1) and the postulated transient. Also the crack loading of the postulated cracks will be analyzed along the crack front. For each crack a fracture assessment is performed concerning crack initiation in the sense that a maximum allowable RT_{NDT} is determined.

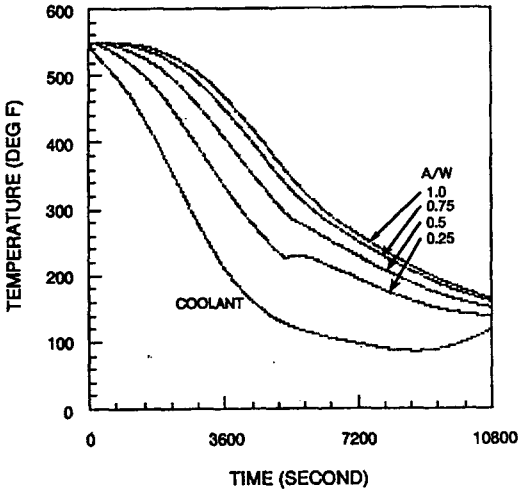

Fig. 6. Temperature Histories of the Vessel Wall

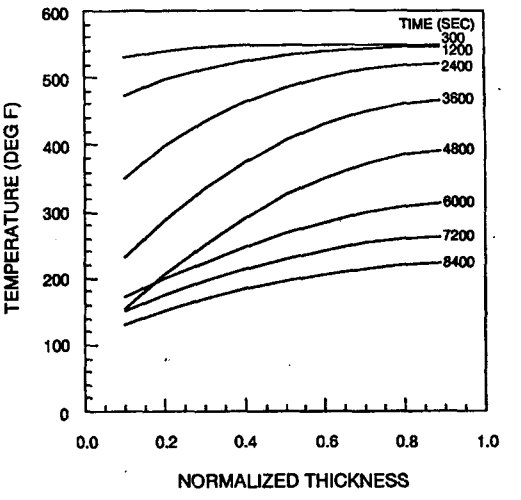

Fig. 7. Temperature Distributions Through the Vessel Wall

5.2. Results and Discussion

The temperature distribution in the vessel wall is calculated from the coolant temperature variations during the transient. Figure 6 shows the temperature histories of the vessel wall at a / w = 0.25, 0.5, 0.75 and 1.0 locations. Figure 7 shows the temperature distributions in the vessel wall. The hoop and axial stress distributions versus time are shown in Figure 8, and their distribution through the vessel wall are shown in Figure 9.

Using the equations (17), (18) and (19), the K_I, K_{IC} and K_{IA} variations through the thickness are determined for each time step during the transient. Their distributions at several time step are shown in Figures 10 and 11 for axial and circumferential cracks, respectively. For a typical result at time = 3600 seconds in Figure 10, there are two regions where K_I exceeds K_{IC} : a / w = 0.0192 to 0.3867 (transient behavior), and a / w = 0.688 (upper shelf behavior). There is also an arrest point a / w = 0.0128. A summary of all initiation and arrest points for all times is shown in the critical crack depth diagram as shown in Figures 12 and 13 for axial and circumferential cracks, respectively. For the axial crack with aspect ratio of 1/6 and fluence of f = 3.5 (Figure 14), the minimum crack size for initiation is a / w = 0.0182.

In the warm prestress analysis, the K_I variation with time is determined for each crack depth considered and is shown in Figures 12 and 13 for axial and circumferential cracks, respectively. For the axial crack with aspect ratio of 1/6, the maximum K_I values 70.0 and 108.4 ksi$\sqrt{\text{in}}$ occur at 3795 (θ_{max} = 3795) and 3675 (θ_{max} = 3675) seconds for a / w = 0.1 and a / w = 0.4, respecti-vely. Even though K_I value exceeds K_{IC} for this crack depth, there is no initiation beyond this point θ_{max} because K_I is falling. A summary of θ_{max} for each crack depth is also included in the critical crack depth diagram (Figures 12 and 13). Figure 14 shows two typical critical crack depth diagrams for the axial crack with aspect ratio of 1/6 and fluences of 3.5 and 0.5. For the case of f = 3.5, the range of the crack sizes which can be initiated is

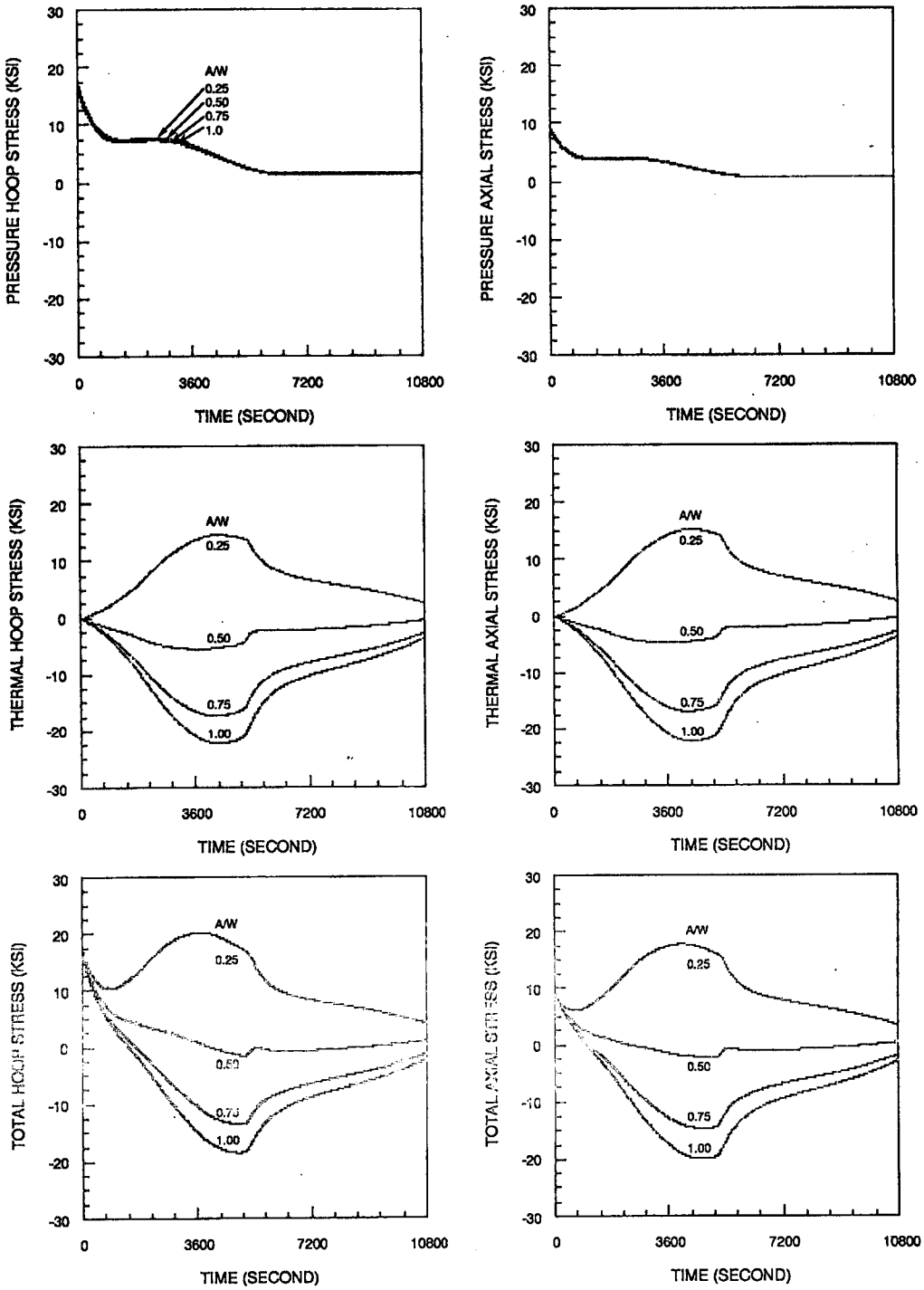

Fig. 8. Hoop and Axial Stress Histories of the Vessel Wall

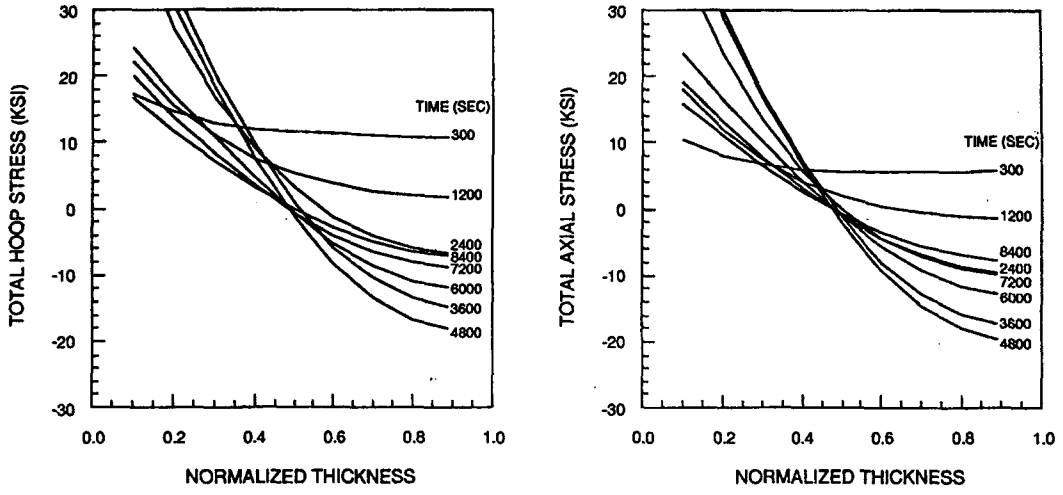

Fig. 9. Stress Distributions Through the Vessel Wall

a / w = 0.021 to 0.41, compared with a / w = 0.018 to 0.70 by standard analysis. Therefore, according to the warm prestressing analysis, a flaw greater than a / w = 0.021 would be required for initiation. In f = 0.5, the initiation curve is encompassed by the arrest curve, which means that all initiated cracks are arrested and therefore there is no through-wall cracking during the transient.

To get a maximum allowable RT_{NDT} for crack with a / w = 0.06 not to be initiated, several analyses are performed with respect to the fluence. If the fluence is determined, the RT_{NDT} is calculated from equations (20), (21), and (22) as follows :

$$RT_{NDT} = RT_{NDT0} + CF \times (f_{surf}\, e^{-0.24a})^{0.28-0.101 \log(f_{surf} e^{-0.24a})} \quad (23)$$

The chemistry factor CF determined from Regulatory Guide 1.99, Rev.2 [8] for the given contents of copper and nickel in Table 1 is 217.25 °F, and RT_{NDT0} is 20 °F. Therefore equation (23) at the inside vessel surface a = 0.0 becomes

$$RT_{NDT} = 20 + 217.25 \times (f_{surf})^{0.28-0.101 \log(f_{surf})} \quad (24)$$

From the critical crack depth diagrams as shown in Figures 12 and 13 for axial and circumferential cracks, the maximum fluence for crack with a / w = 0.06 not to be initiated is determined and is shown in Figure 15, and the corresponding RT_{NDT} is also shown on the same figure. The maximum allowable RT_{NDT} is 136.7 oF for axial crack of 1/6 aspect ratio. Generally axial crack is found to be more severe than circumferential crack. Also it is shown in Figure 15 that the orientation of crack is not significant for the aspect ratio of less than 1/4.

6. Conclusions

An analysis program for the evaluation of pressure vessel integrity under pressurized thermal shock is developed. For given material properties and transient history such as temperature and pressure, the stress distribution is calculated and then stress intensity factors are obtained for a wide range of crack sizes. The stress intensity factors

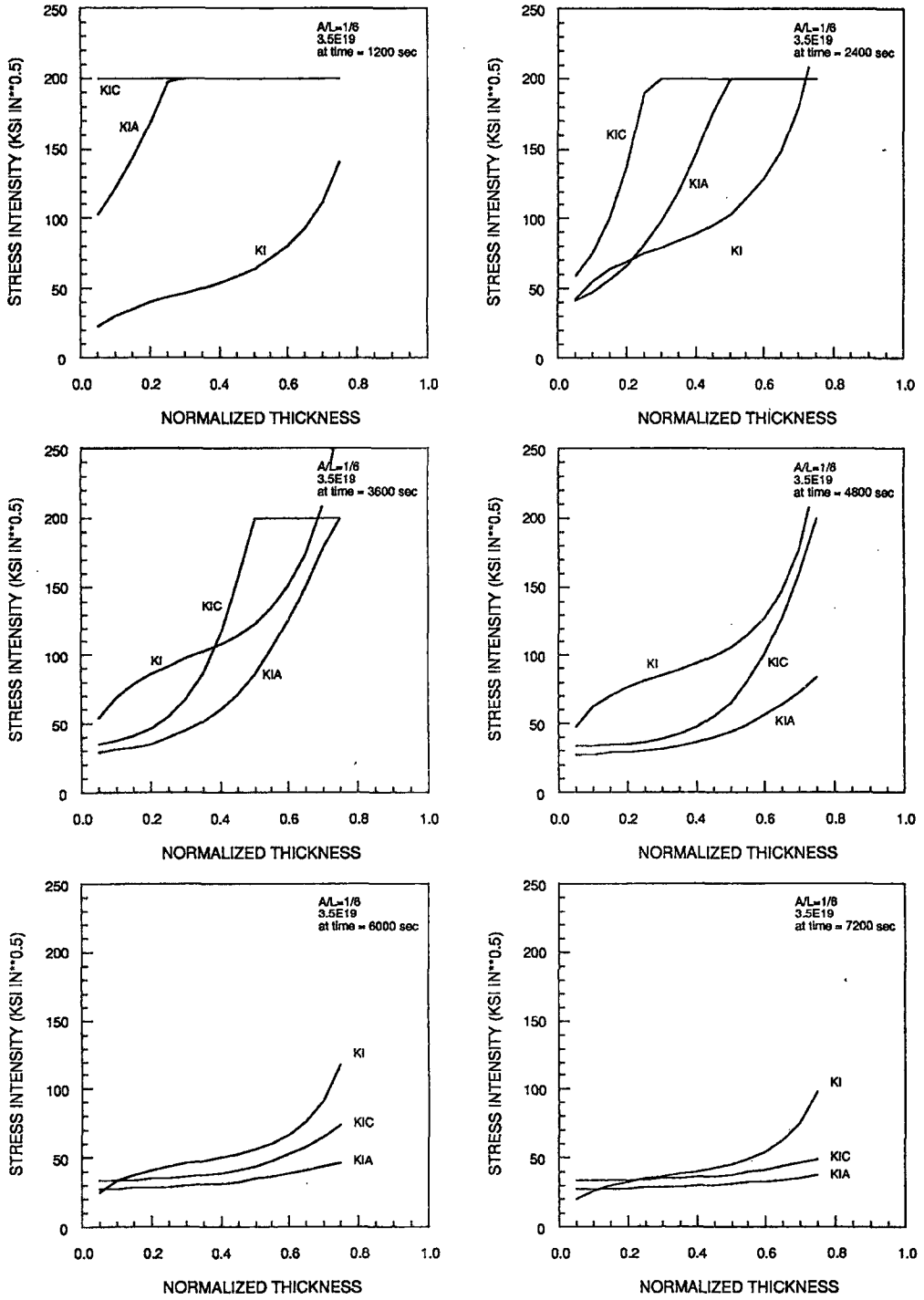

Fig. 10. Determination of Critical Crack Sizes for Axial Crack

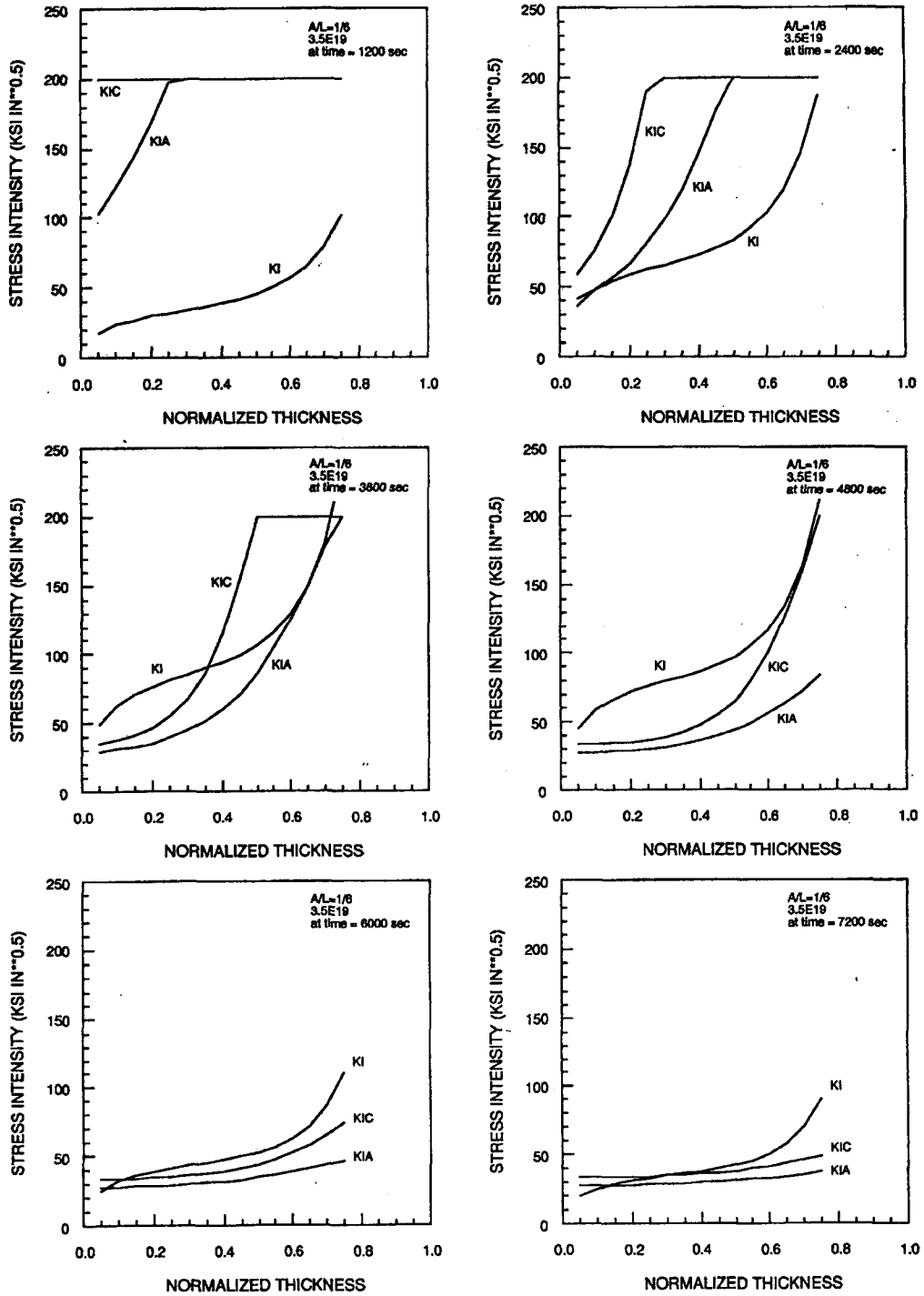

Fig. 11. Determination of Critical Crack Sizes for Circumferential Crack

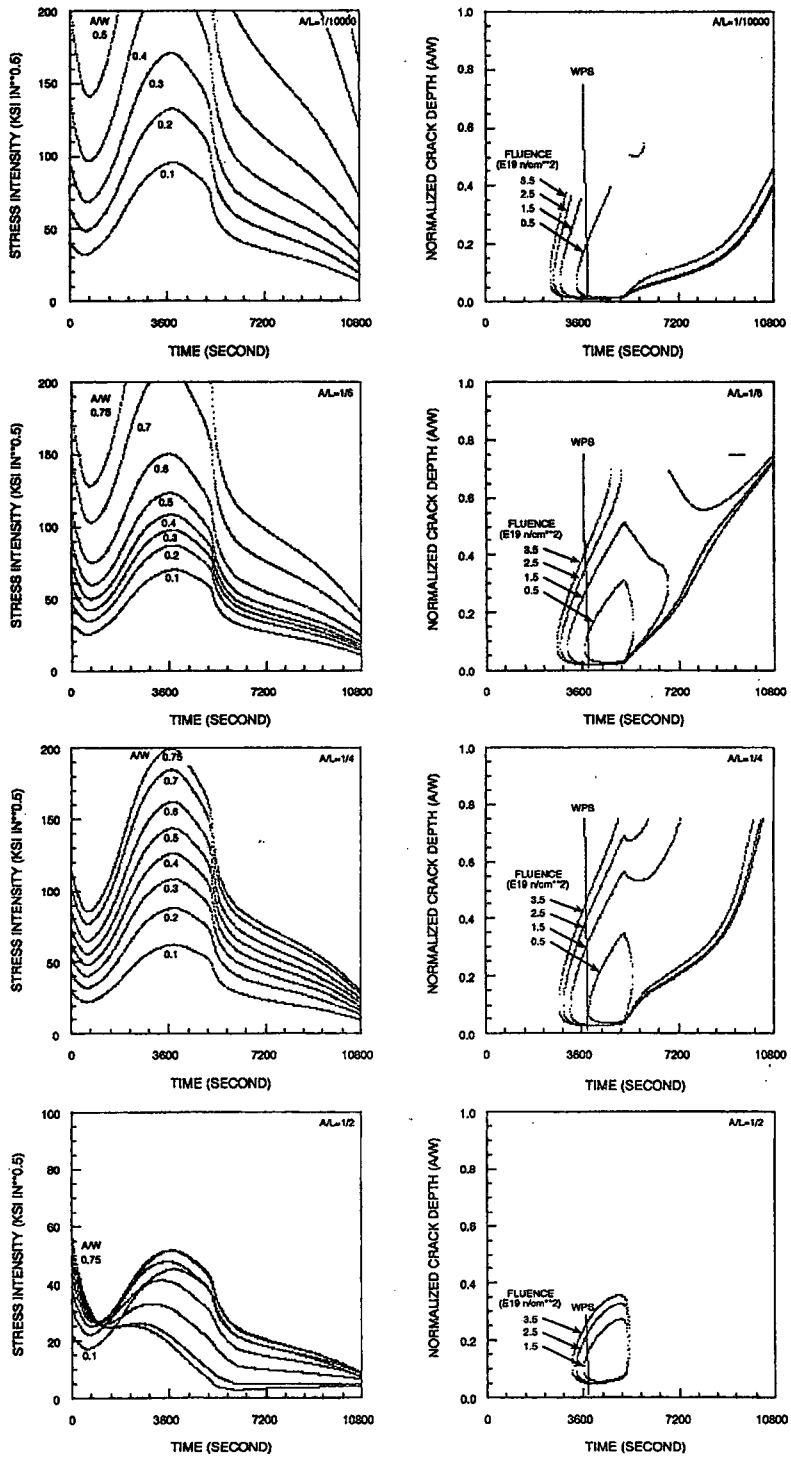

Fig. 12. Stress Intensity Plots and Critical Crack Depth Diagrams for Axial Crack

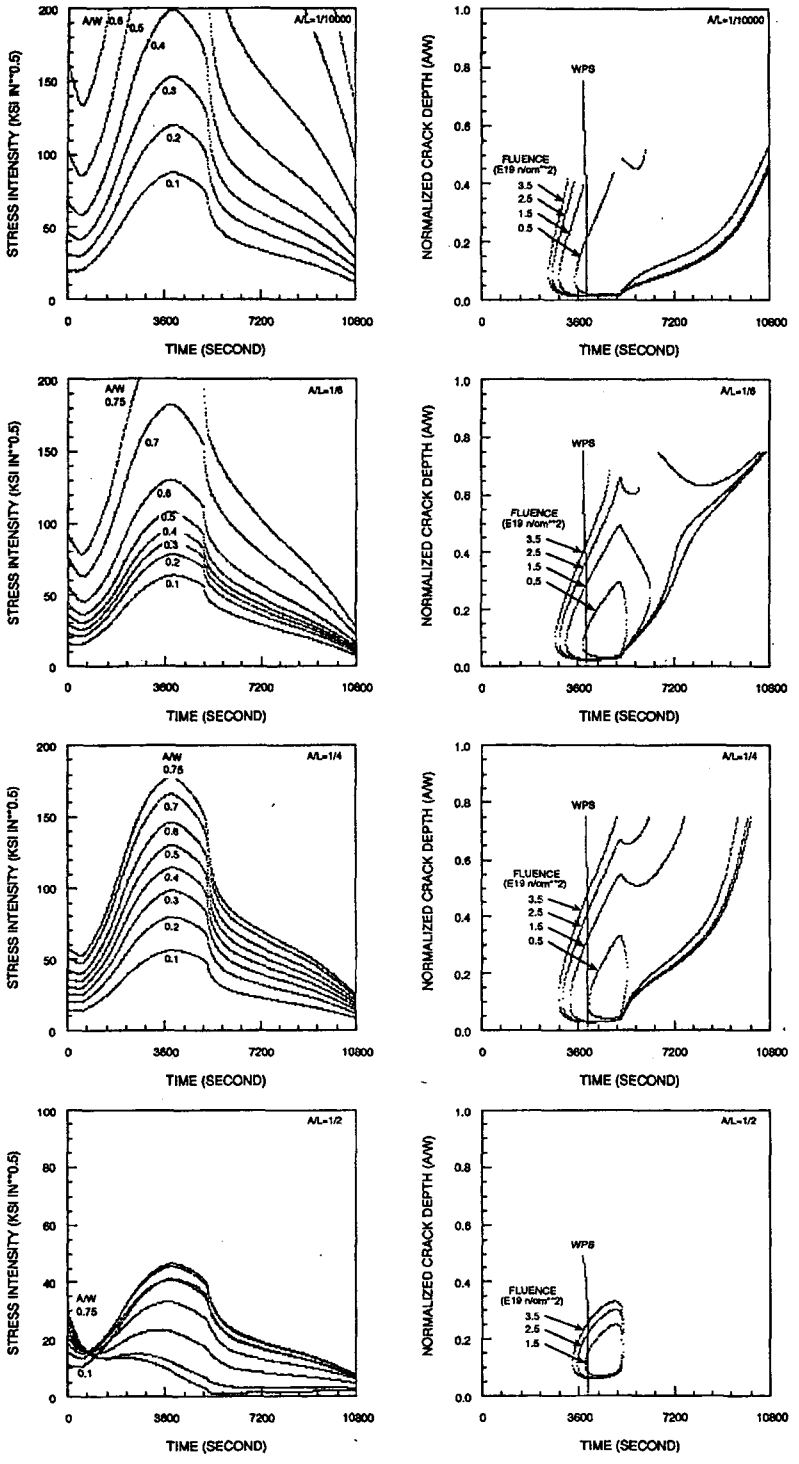

Fig. 13. Stress Intensity Plots and Critical Crack Depth Diagrams for Circumferential Crack

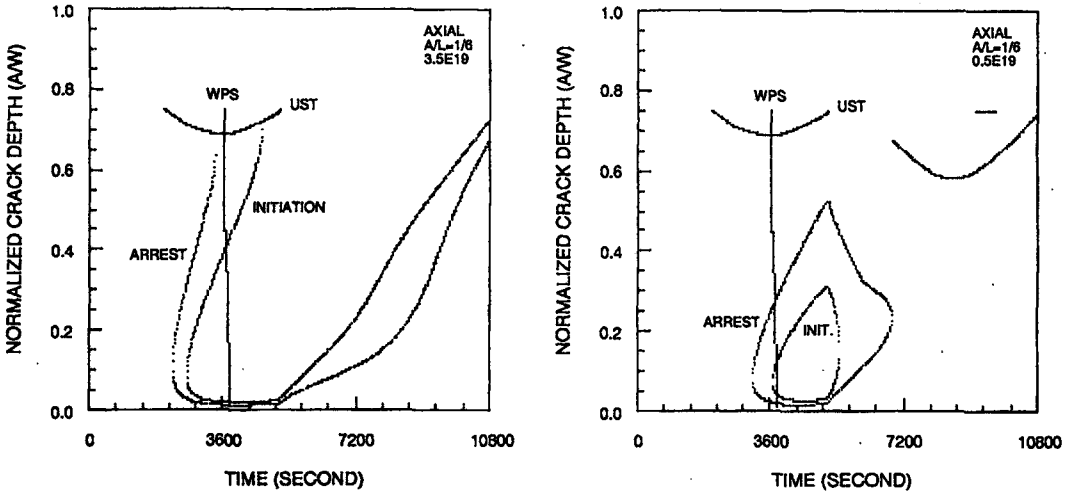

Fig. 14. Critical Crack Depth Diagrams for Axial Crack (a/l = 1/6)

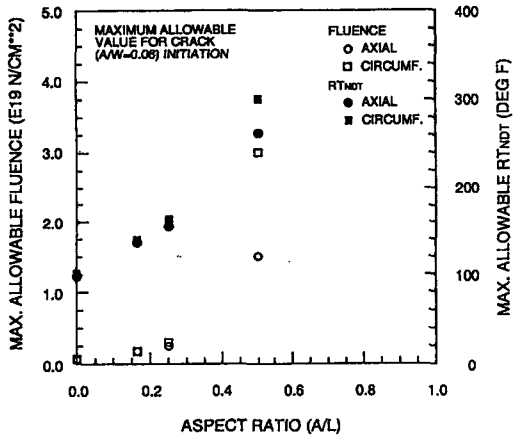

Fig. 15. Maximum Allowable Fluence and RT_{NDT} for Crack to be Initiated

are compared with the fracture toughness to check if cracking is expected to occur during the transient.

A round robin problem of PTS during a small break loss of coolant transient has been analyzed as a part of the international comparative assessment study, and the evaluation results are discussed. The allowable maximum values of RT_{NDT} are determined for various crack sizes and it is found that axial crack is more severe than circumferential crack. Also the direction of crack is not significant for the aspect ratio of less than 1/4.

Structural integrity of the pressure vessel in view of PTS may be evaluated using the analysis program developed in this study. Especially for the life extension of the old plant, this program can be used.

References

1. Oezisik, M.N., *Heat Conduction*, John Wiley & Sons, (1980)
2. Myers, M.N., *Analytical Method in Conduction Heat Transfer*, McGraw- Hill, New York, (1971)
3. ASME, *ASME Boiler and Pressure Vessel Code*, Section III, Appendix I, (1989)
4. Timoshenko, S.P. and Goodier, J.M., *Theory of Elasticity*, 3rd ed., McGraw-Hill, New York, (1970)
5. Harvey, J.F., *Theory and Design of Modern*

Pressure Vessels, 2nd ed., Van Nostrand Reinhold Co., New Jersey, (1960)

6. ASME, *ASME Boiler and Pressure Vessel Code*, Section XI, Appendix A, (1989)
7. Marston, T.U., *Flaw Evaluation Procedures : ASME Section XI*, EPRI NP-719-SR, EPRI, (1978)
8. USNRC, "Radiation Embrittlement of Reactor Vessel Materials," Regulatory Guide 1.99, Rev.2, US Nuclear Regulatory Commission, May (1988)
9. McGowan, J.J., "Application of Warm Prestressing Effects to Fracture Mechanics Analyses of Nuclear Reactor Vessels during Severe Thermal Shock," *Nuclear Engineering and Design*, Vol.51, 1979, pp.431-444.
10. Curry, D.A., "A Model for Predicting the Influence of Warm Pre-stressing and Strain Ageing on the Cleavage Fracture Toughness of Ferritic Steels," *International Journal of Fracture*, Vol.22, 1983, pp.145-159.
11. OECD/NEA PWG-3, "Reactor Pressure Vessel Pressurized Thermal Shock International Comparative Assessment Study," GRS mbH, December 23, (1996)